

# A phenotype-structured model for the tumour-immune response

Zineb Kaid, Camille Pouchol, Jean Clairambault

January 16, 2023

## Abstract

This paper presents a mathematical model for tumour-immune response interactions in the perspective of immunotherapy by immune checkpoint inhibitors (*ICIs*). The model is of the integro-differential Lotka-Volterra type, in which heterogeneity of the cell populations is taken into account by structuring variables that are continuous internal traits (aka *phenotypes*) representing a lumped “aggressiveness”, i.e., for tumour cells, ability to thrive in a viable state under attack by immune cells or drugs - which we propose to identify as a potential of de-differentiation -, and for immune cells, ability to kill tumour cells. We analyse the asymptotic behaviour of the model in the absence of treatment. By means of two theorems, we characterise the limits of the integro-differential system under an *a priori* convergence hypothesis. We illustrate our results with numerical simulations, which show that our model exemplifies the three *Es* of immunoediting: elimination, equilibrium, and escape.

**Keywords:** Tumour-Immune interactions, Phenotype-structured model, Asymptotic analysis, Immune checkpoint inhibitors

## 1 Introduction

Cancer is one of the leading causes of death in the world. Several clinical and experimental studies have confirmed that the immune system plays a decisive role, providing tumour control, long-term clinical benefits and prolonged survival [24]. Nevertheless, the anti-tumour immune response is an extremely complex process that depends on many factors. In this context, mathematical models could help understand the interactions between tumour growth and the immune response.

The model presented below has been designed to analyse by integro-differential equations tumour-immune interactions between cell populations and the asymptotic behaviours of these populations. We follow the principle of modelling cell population heterogeneity by structuring them by relevant internal traits (aka cell *phenotypes*), as initiated in [13] and partially reviewed in [6].

Phenotype-structured models, which are usually stated in terms of non-local partial differential equations or integro-differential ones have been widely used to describe phenotype heterogeneity in tumour cell populations. In these models, the phenotypic state is represented by a continuous real variable  $x$ , modelling different biological characteristics such as viability and fecundity, see [2,3,12,18] and the references therein.

To the best of our knowledge, the first phenotype-structured model for tumour-immune interactions was proposed by Delitala and Lorenzi [7], where a tumour cell population characterised by heterogeneous antigenic expressions is exposed to the action of antigen-presenting cells and immune T-cells. More precisely, their model incorporates five populations of cells. All populations but one are assumed in [7] to be structured by a real continuous variable in  $[0, 1]$  representing an internal phenotypic state of the cell. Their model reproduces well the selective recognition and learning processes in which immune cells are involved. Our model, which belongs to the category of non-local Lotka-Volterra systems, has been designed to offer a rationale for the use of immune checkpoint inhibitors [22].

Such models, which can be derived from stochastic individual-based models [5], are known to possibly lead to the concentration of populations on one or several phenotypes, which will be shown in the model described below for the tumour cell population, under restrictive assumptions. The original motivation

for this work is the article [18], in which an integro-differential system for the time evolution of densities of cancer and healthy cells, structured by a continuous phenotypic variable, representing their level of resistance to chemotherapy to which they are exposed is studied. In a completely different context, which is the application to *ICI* immunotherapy, we will here make use of similar methods of asymptotic analysis.

**Main theoretical and numerical results.** In summary, we derive an implicit formula to compute the possible (generally unique) non-trivial limits the solution to the integro-differential system may have. More precisely, under the strong *a priori* assumption that the density of cancer cells converges, we prove that its limit is a weighted Dirac mass. We provide in Section 4 a formula to compute the weight and location.

Moreover, we present simulation results that show how our model illustrates the three *Es* of immunoediting (elimination, equilibrium, and escape) and that it may also exhibit oscillatory solutions. We mention that, in the context of our model, which is of the Lotka-Volterra type, it is difficult to distinguish between equilibrium and escape. Nevertheless, we propose to interpret solutions for which the system reaches its carrying capacity as tumour escape, whereas solutions for which the tumour cell population is contained below its carrying capacity may be interpreted as an equilibrium between tumour and immune cells.

**Outline of the paper.** The paper is organised as follows. In Section 2, we start by introducing biological motivations for the development of the model under study. The integro-differential model itself is presented in detail in Section 3. We then analyse the model and prove some asymptotic properties in Section 4. In Section 5, we present some numerical results. In Section 6, we conclude with several comments and open questions.

## 2 Biological background

When a cancer cell population thrives, the immune response, and essentially its part that is constituted of CD8+ T-lymphocytes (for the adaptive response) and NK-lymphocytes (for the innate response), consists of recognising as foe elements and killing these cancer cells. This has been called immunosurveillance, later immunoediting [4, 20, 22], which may consist of three different configurations: eradication, equilibrium or escape (see Figure 1). If this process is performed during the early stages of tumour initiation, the tumour is quickly and successfully eradicated. However, cancer cells can escape these innate NK-cell and adaptive specific T-cell immune responses in the course of genetic and phenotypic evolution at the time scale of a cancer disease. More precisely, phenotypic<sup>1</sup> heterogeneity in the cancer cell population, involving its possible internal invasion by secondarily mutated, robust, cells, may be responsible for both tumour escape and treatment failure. Here, a focus is set on immunotolerance [20, 22], which renders cancer cells able to evade immune detection and elimination. Indeed, cancer cells have the resource to weaken the immune response by emitting molecules such as PD-L1 (i.e., PD-1 ligand) and CTLA-4<sup>2</sup> which can respectively bind to the PD-1 and B7 receptors on activated T-cells, inhibiting their cytotoxic activity and reducing their own immunogenicity. This is represented in the model by direct competition between cancer cells and T-lymphocytes. As regards innate immunity, the role of NK-lymphocytes (readily effective on cancer cells with lacking MHC-I surface antigens [15], not the same mechanism as in the case of CD8+ T-cells, that are activated by tumour antigen-presenting cells, APCs), has recently gained more consideration, in particular, because a role for anti-PD1/anti-PDL1 has been suspected for them in cancer immunotherapies [17].

---

<sup>1</sup>The term phenotype means here the set of observable characteristics of an individual (a cell, represented by a population density function taking a given value, in our model), resulting from the interaction of its genotype with the environment; observable characteristics are not necessarily visibly observed but may be internal traits, e.g., related to some epigenetic, reversible, modification by a graft of a chemical radical (methyl, acetyl...) on some base of the DNA before transcription or on some amino acid in a histone protein, such traits being possibly evidenced after some dynamic stimulation only.

<sup>2</sup>PD-1: programmed cell death protein 1/CTLA-4: cytotoxic T lymphocyte antigen 4 for the adaptive response.

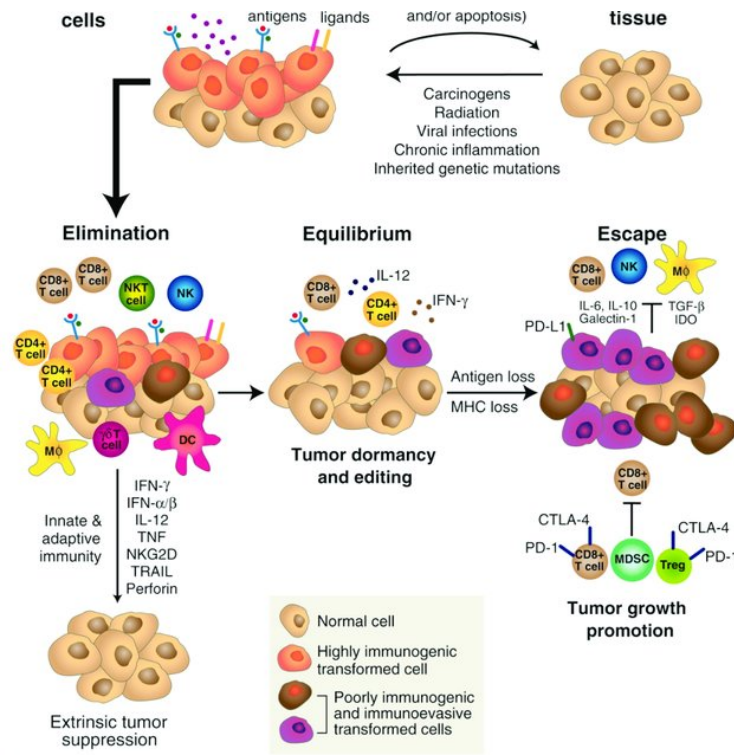


Figure 1: The cancer immunoediting process after R. D. Schreiber, Science 2011 [22]. It proceeds according to three possible situations termed elimination, equilibrium and escape. In the present mathematical framework of our model, we classify the different outcomes of the tumour-immune interactions according to the levels of the tumour population density values (as compared to the theoretical and numerical values of the tumour carrying capacity), themselves dependent on the parameters of the activation term by the APCs towards T-cells in lymphoid organs (specificity of the immune response) or by humoral messages sent by patrolling NK-cells to resident NK-cells in lymphoid organs or tissues to favour their proliferation (innate, non-specific immune response).

Immunotherapy with immune checkpoint inhibitors [22] (hereafter noted *ICIs*) is a recently introduced class of drugs (aiming at being less toxic than the classical anti-cancer therapies, chemotherapy and radiation therapy) that inhibit such cancer cell-produced inactivation of T- and NK-lymphocytes, either at the receptor sites on lymphocytes or by inhibiting the ligands themselves. The clinical use, firstly of anti-CTLA4 drug Ipilimumab, which has been shown to mainly target the priming lymphocyte response at the level of lymphoid organs [27], and later of direct (at the tumour site) antagonisers of PD-L1 to PD-1 binding, drugs Nivolumab and Pembrolizumab [8]<sup>3</sup>, has drastically modified the prognosis of several advanced cancers that were until recently out of reach (e.g., melanoma, a skin cancer with very bad prognosis [21]), offering sustained positive responses (about 20% of complete cures, the remaining 80% consisting of non- or partial responders with relapse). However, not all cancer types respond as well as melanoma. To the best of our knowledge, the reasons for successes or failures are still unknown. Moreover, there is no clear dose-response relationship and a maximum tolerated dose, for checkpoint inhibitors, has not been identified as yet [11].

<sup>3</sup>Note that in the sequel, as our model aims at representing direct tumour-immune interactions and their possible enhancing by immunotherapy, the term *ICIs* should be thought of as representing this second class of drugs.

### 3 The model

#### 3.1 The cell populations

To describe tumour-immune interactions, we consider three different cell population densities:

- a heterogeneous cancer cell population  $n(t, x)$  with continuous aggressiveness (or malignancy) trait  $x \in [0, 1]$  linked to their stemness (i.e., their ability to de-differentiate, allowing them to re-differentiate with adapted phenotypes);
- a heterogeneous population of mixed competent T-lymphocytes and NK-lymphocytes  $\ell(t, y)$  endowed with continuous anti-tumour aggressiveness trait  $y$  ranging from 0 (exhausted) to 1 (highly aggressive) interacting with cancer cells  $n(t, x)$  at the tumour site;
- a heterogeneous population of naive T-lymphocytes and patrolling NK-lymphocytes  $p(t, y)$ , either resident and present at the tumour site (for NK-cells, particularly activated by their sensing lack of MHC-I surface antigens in tumour cells, so-called “loss-of-self”), or present in distant lymphoid organs, informed there by **APCs** (antigen-presenting cells, here represented by a weighted integral of the cancer cell population involving a localisation kernel coupling  $x$  and  $y$ ) of the number and malignancy  $x$  of the cancer cell population. Both “naive” cell populations are represented by the lumped population density  $p(t, y)$ . Note that in simulations, we will consider separately the three cases: innate, adaptive, and a combination of the two immune responses.

Our model is given by the following system of integro-differential equations (IDEs):

$$\begin{cases} \frac{\partial n}{\partial t}(t, x) = [r(x) - d(x)\rho(t) - \mu(x)\varphi(t)] n(t, x), \\ \frac{\partial \ell}{\partial t}(t, y) = p(t, y) - \left( \frac{\nu(y)\rho(t)}{1 + hICI(t)} + k_1 \right) \ell(t, y), \\ \frac{\partial p}{\partial t}(t, y) = \chi(t, y)p(t, y) - k_2 p^2(t, y). \end{cases} \quad (3.1)$$

with the total number of cancer cells at time  $t$

$$\rho(t) := \int_0^1 n(t, x) dx. \quad (3.2)$$

The initial value function  $n(0, x)$  is chosen to represent the assumed initial malignancy of the tumour, and in the same way, the initial value functions  $\ell(0, y)$  and  $p(0, y)$  will be chosen to represent the initial host’s immune response.

#### 3.2 Biological motivations

In the above model:

- For the tumour cell population of density  $n(t, x)$ , a cell of phenotype  $x$  is all the more malignant, i.e., able to thrive, as  $x$  is closer to 1, and conversely less malignant when  $x$  is close to 0. More particularly, the malignancy trait  $x$  represents a progression potential towards stemness (ability to differentiate).

Let us mention that the malignancy trait  $x$  might in principle be measured in single cells by assessing the expression of genes like the Yamanaka genes, identified in 2006, that enable dedifferentiation [25]. More recently, a de-differentiated phenotype  $MIT^{low}/AXL^{high}$  phenotype, defined by the concomitant downregulation of the transcription factor  $MIT$  and accumulation of the tyrosine kinase receptor  $AXL$  has been evidenced in immunotherapy-resistant melanoma cells [10], which could provide a measurable basis for such continuous malignancy trait  $x$  identified as a potential

for tumour cells to de-differentiate in response to deadly attacks coming from the immune response or more generally from the tumour microenvironment, including drugs. Importantly, we assume in this model that both the density of a loss-of-self sensed by NK-cells in tumour cells (recalled in next paragraph) and the density of tumour antigens sensed by APCs reflect the level of the *hidden* tumour aggressivity phenotype  $x$  in the tumour cell population, even though the anti-tumour action of lymphocytes will be directed towards the *manifest* loss-of-self and tumour antigen-bearing cells.

- For the T-lymphocyte population and for the non-adaptive NK-lymphocyte population, in a similar way, we structure it by a phenotype  $y$  of anti-tumour aggressiveness, which may be defined as the reverse of the ‘dysfunction’ or ‘exhaustion’ phenotype that has been observed in CD8<sup>+</sup> T-cells exhibiting incapacity to efficaciously fight tumour cells. In our model, the difference between NK-lymphocytes and effector (CD8<sup>+</sup>) T-cells consists in the nature of their action on tumour cells, either independent of the tumour phenotype  $x$  for NK-cells represented below by a function  $\varphi(t)$ , or highly dependent on it for T-cells, represented by a function  $\varphi(t, x)$ . In the analysis of our model, we will study separately the case of innate (function  $\varphi(t)$ ) and adaptive (function  $\varphi(t, x)$ ) immune response (and also a mix of these two cases in our simulations). To identify and measure in single cells such dysfunction or exhaustion in T-cells, different biological markers have been proposed; they have been recently reviewed in [26] (an article in which it is, in particular, noted that “*T cell dysfunctionality is a gradual, not a binary, state*”, which fully justifies the continuous character of our structure variable  $y$ ). The closer the phenotype  $y$  approaches 0, the less aggressive are T- and NK-lymphocytes, i.e., less competent to kill cancer cells (complete exhaustion), whereas if  $y$  approaches 1, they are highly aggressive (full competence) against the targeted tumour cells, as identified by their competence as immune cells due to the tumour antigen recognition performed by the APCs, or to the absence of MHC-I antigens (loss-of-self) in tumour cells in the case of NK-cells. The principle of immune checkpoint inhibition (*ICI*) immunotherapy is to boost CD8<sup>+</sup> T-lymphocytes and NK-lymphocytes in their efficacy by antagonising such tumour-emitted inhibitory mechanisms, mainly in the modelling framework presented here, PD-L1 to PD-1 binding on T-cells and NK-cells.

### 3.3 Modelling choices for the mathematical functions of phenotypes

In the absence of experimental data, the precise choices for functions  $r, d, \mu, \nu, \psi$  are largely arbitrary, only guided by physiological considerations on an assumed monotonicity. They are listed in Table 1 of Section 5 for simulations, reflecting such monotonicity: non-increasing for  $r, d, \mu, \nu$ , non-decreasing for  $\psi$ . The biological background for these functions is as follows.

- We assume that in the absence of immune response, tumour cells undergo logistic growth, with a net growth rate (aka fitness) defined by

$$r(x) - d(x)\rho(t). \tag{3.3}$$

Here, the function  $r(x)$  stands for the intrinsic proliferation rate. As  $x$  stands for a de-differentiation, stem-like, cell phenotype, admitting that a stem-like status does not favour replication velocity,  $r$  will typically be assumed to be a positive, decreasing function of  $x$  on  $[0, 1]$ , e.g., of the form

$$r(x) = r_0 - \eta x^2, \tag{3.4}$$

where the parameter  $r_0 > 0$  corresponds to the maximum fitness of cancer cells, while  $\eta > 0$  provides a measure of the strength of natural selection in the absence of the immune response. The term  $d(x)\rho(t)$  models the intrinsic death rate due to within-population competition for space and resources, assumed to be proportional to the total population number of tumour cells  $\rho(t)$ . The function  $d$  will typically be taken to be positive, decreasing function of  $x$  on  $[0, 1]$  (in the same way as for the replication function  $r$ , a de-differentiated, stem-like, status is admitted to protect cells from the natural death term represented by the function  $d$ ).

The fitness structure chosen here for the tumour and for the immune cell population is of the nonlocal Lotka-Volterra type. It has been in particularly used in [16] to model the adaptation of individuals to their environment.

- We assume that, once an immune response has been activated, the tumour cells interact with competent T-cells and NK-cells at a rate which is proportional to the product of the tumour cell population density by a weighted integral  $\varphi(t)$  given by

$$\varphi(t) = \int_0^1 \psi(y)l(t,y)dy, \quad (3.5)$$

where  $\psi$  is a positive function, which we will typically take to be increasing on  $[0,1]$ . The term  $\mu(x)\varphi(t)$  models an additional death rate for tumour cells due to their interactions with competent T cells  $\ell$ . We note that in this formulation, the immune response  $\varphi(t)$ , emitted by NK-cells present at the tumour site, is non-specific, only the tumoral sensitivity function  $\mu(x)$  makes it somehow specific; the function  $\varphi(t)$  then stands for a response in which the phenotype  $y$  in lymphocytes is averaged over all the population of competent T-cells,  $\varphi(t)$  representing a sort of “mass immune response”. In order to account for an adaptive immune response which is the one of T-cells, one must more generally consider  $\varphi$  to be of the form  $\varphi(t,x) = \int_0^1 \psi(x,y)\ell(t,y)dy$  (note that the weight function  $\psi$  in the adaptive case depends on both  $x$  and  $y$ ). We will in the sequel consider separately these two cases, native non-specific (NK-cells:  $\varphi(t)$ ) and adaptive specific (T-cells:  $\varphi(t,x)$ ) anti-tumour immune response (and also a mixed case in our simulations).

- The function  $\mu$  of  $x$  represents a factor of sensitivity to the effects of the immune response. As de-differentiation is supposed to protect tumour cells from these effects (e.g., by hiding tumoral antigens, targets of lymphocytes),  $\mu$  is chosen to be a positive, decreasing function of  $x$ .
- The amplification of the naive T-lymphocytes  $p(t,y)$  at lymphoid organs is related to the mean  $x$  malignancy value through a weighted integral  $\chi(t,y)$  of the tumour cell population, representing the message borne by APCs to initiate the adaptive anti-tumour immune response produced in the lymphoid organs. When an APC detects a tumour cell, the related antigen is presented to naive T-cells. Thus, those naive T-cells that recognise this antigen as their cognate one become activated. Activated T cells start to proliferate and, through a complex process chain, they become able to recognise and attack tumour cells that express the cognate antigen. The function  $\chi(t,y)$  is defined as

$$\chi(t,y) = \int_0^1 \omega(x,y)n(t,x)dx, \quad (3.6)$$

where for instance,  $\omega(x,y) = \alpha \frac{1}{s} e^{-|x-y|/s}$ , so as to represent a more or less faithful message transmitted by the APCs to the lymphoid organs about both the size and the aggressiveness of the tumour. The efficacy of T cells in killing tumour cells depends on the initial size of the tumour and on how localised the kernel is (i.e., on the width of the range of phenotypes  $y$  concerned by their detected tumour cognates  $x$ , which can be measured by the value of the parameter  $s$  in the proposed function  $\omega(x,y)$ ). The parameter  $\alpha$  represents the strength of the immune response (i.e., a good transmission by APCs and a good synthesis of the expansion). In the present model, APC communication between recognition at the contact of tumour cells and activation of naive lymphocytes at the site of lymphoid organs is represented, for the sake of simplicity without taking communication time into consideration, by the shortcut of the function  $\omega(x,y)$ .

- We consider a similar mechanism for NK-lymphocytes, that are known to proliferate and amplify not only in the bone marrow but also in lymphoid organs, like T-lymphocytes [1]. In the case of this innate immune response, there are no APCs, but the message from sensor patrolling NK-lymphocytes to proliferating NK-lymphocytes is assumed to be of (coarse, quantitative) humoral nature.

- In the second equation of (3.1) for the competent T-lymphocytes  $\ell(t, y)$ , the function  $\nu$  of the anti-tumour aggressiveness phenotype  $y$  represents the weakening (immunotolerance) of T-lymphocytes induced by PD-1 ligands; note that it is assumed to be decreased by *ICIs*. As the function  $\nu$  stands for a sensitivity factor in lymphocytes to the weakening reaction molecules (in this model, mainly PD-L1) emitted by tumour cells or produced in the tumour microenvironment, it will typically be chosen to be a positive, decreasing function of  $y$ , which in this case reflects the fact that cells in the phenotypic state  $y = 1$  are fully aggressive on contact with tumour cells and, for cells in phenotypic states other than the most aggressive one, the inhibition term induced by the tumour cells decreases with the drug dose.
- The parameter  $k_1$  stands for the natural death rate of the population of competent T- and NK-lymphocytes.
- The input of external control targeting immune checkpoints inhibitors is represented by the function  $ICI(t)$  that enhances anti-tumour CD8+ T-lymphocyte and NK-lymphocyte responses by boosting the exhausted immune cells, which helps them to respond more strongly to the presence of the tumour, by “weakening the weakening” due to immunotolerance induced by the tumour cells. We assume that

$$0 \leq ICI(t) \leq ICI^{max}. \quad (3.7)$$

for some maximum tolerated dose  $ICI^{max}$ . The factor  $\frac{1}{1+hICI(t)}$ , with  $h > 0$ , models the decrease in the immunotolerance rate due to the immune checkpoints inhibitors therapy. We note that fine details of clinical administration protocols are not meant to be described here. We also mention that  $ICI$  is a quantitative dose function, and is APC-independent.

- The term  $-k_2 p(t, y)$  with the positive constant  $k_2$  stands for the self-limitation on population growth imposed by carrying capacity constraints (e.g., limited availability of space and resources in lymphoid organs).

### 3.4 Goals of the present study

Our goals in this study are

- to study the asymptotic properties of the model, as we want to understand how the interaction between tumour cells and T cells leads to the selection (or not) of some traits, which are considered as dominant traits by the environment;
- to numerically investigate if and how our model captures the three *Es* of immunoediting, i.e., eradication, equilibrium and escape.

In order to exploit useful ideas to guide our study of the dynamics of the above integro-differential system, we mention that a simplified version of (4.10) has been analysed in [9]. Assuming that all functions are constant in  $x$  and  $y$ , and denoting

$$\sigma(t) := \int_0^1 \ell(t, y) dy, \quad \text{and} \quad \gamma(t) := \int_0^1 p(t, y) dy, \quad (3.8)$$

the system (3.1) boils down to the dynamics of  $(\rho(t), \sigma(t), \gamma(t))$ , which after integration solves the following ODE system:

$$\begin{cases} \frac{d\rho(t)}{dt} = [r - d\rho(t) - \sigma(t)] \rho(t), \\ \frac{d\sigma(t)}{dt} = \gamma(t) - (k_1 + \nu\rho(t)) \sigma(t), \\ \frac{d\gamma(t)}{dt} = \gamma(t) (\rho(t) - k_2\gamma(t)). \end{cases} \quad (3.9)$$

The mathematical analysis of these equations has been performed in [9], in the particular case where  $k_1 = \nu$ . The existence of the steady states has been characterised and analysed with respect to their local asymptotic stability. Regions of the parameter space have also been identified, in which a Hopf bifurcation exists. The ODE system (3.9) reproduces a tumour equilibrium (second situation of the immunoediting process), which corresponds either to a stable steady state or to a stable limit cycle, characterised by a sustained periodic behaviour of alternating growth and decay (without extinction) of both tumour and immune T cells. For particular choices of initial conditions, the ODE model also captures either tumour eradication or tumour immune escape.

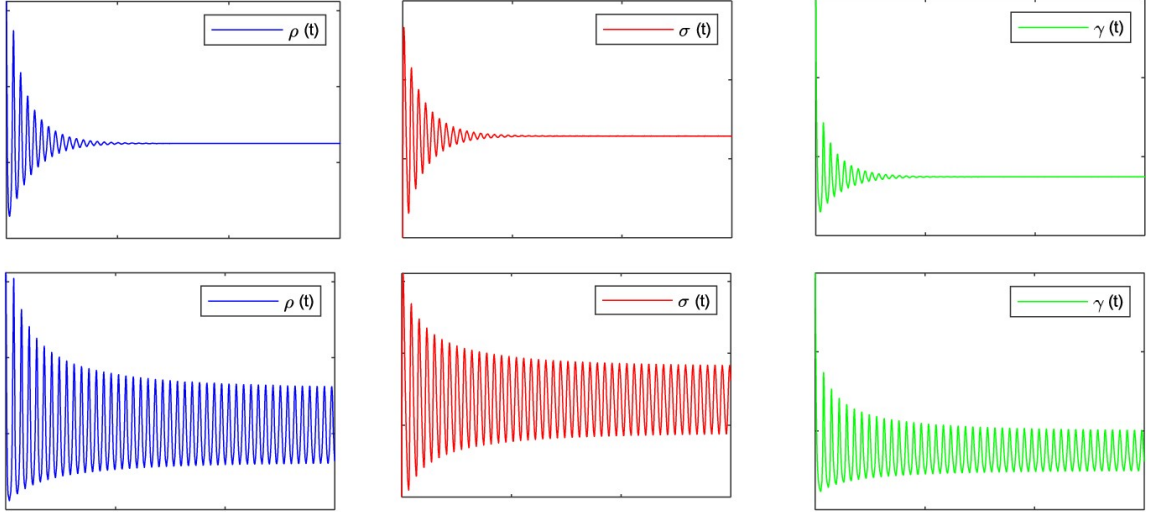


Figure 2: Plots display the time evolution of total masses  $\rho(t)$  (left panel), competent T cells  $\sigma(t)$  (central panel), and naive T cells  $\gamma(t)$  (right panel) as defined by system (3.9) in two different cases: stationary and periodic solutions [9]. **Upper row.** The solution is drawn for the stability of the interior equilibrium  $(0.6257, 1.1436, 0.746)$ , for  $k = 0.8514$ . **Lower row.** The solution is drawn for the instability of the interior equilibrium  $(0.5204, 1.1699, 0.7115)$  with limit cycle (Hopf bifurcation), for  $k = 0.7314$ . For all plots,  $r = 1.3$ ,  $d = 0.25$ ,  $\nu = 0.4$ , and initial conditions are  $(\rho_0, \sigma_0, \gamma_0) = (1.5, 0.5, 3)$ .

## 4 Asymptotic analysis

### 4.1 Asymptotics in the absence of treatment

We study the asymptotic properties of the system (3.1) in the absence of treatment, i.e., with  $ICI(t) = 0$ . Of course, upon changing the function  $\nu$ , our study also encompasses the case where the dose  $ICI$  is taken to be constant with time.

The evolution of the population densities is then governed by the following integro-differential system:

$$\begin{cases} \frac{\partial n}{\partial t}(t, x) = [r(x) - d(x)\rho(t) - \mu(x)\varphi(t)]n(t, x), \\ \frac{\partial \ell}{\partial t}(t, y) = p(t, y) - (\nu(y)\rho(t) + k_1)\ell(t, y), \\ \frac{\partial p}{\partial t}(t, y) = \chi(t, y)p(t, y) - k_2 p^2(t, y), \end{cases} \quad (4.10)$$

the above system starting from initial conditions

$$n(0, x) = n^0(x) \geq 0, \quad \ell(0, y) = \ell^0(y) \geq 0, \quad p(0, y) = p^0(y) \geq 0. \quad (4.11)$$

**Main assumptions on the functions and initial conditions.** For the remaining part of this paper, we assume that the initial conditions  $n^0$ ,  $\ell^0$  and  $p^0$  are all in  $\mathcal{C}([0, 1])$ , and whenever necessary, we will assume that

$$n^0 > 0 \quad \text{and} \quad p^0 > 0 \quad \text{on} \quad [0, 1], \quad (4.12)$$

and we will work with the following regularity assumptions:

$$r, d, \mu, \psi, \nu \in \mathcal{C}([0, 1]), \quad \text{and} \quad \omega \in \mathcal{C}([0, 1] \times [0, 1]), \quad (4.13)$$

all the above functions are assumed to be positive.

The existence and uniqueness of global classical (nonnegative) solutions in  $C^0([0, +\infty), L^1(0, 1)^3)$  is standard and follows from the Banach fixed point theorem, see [16].

**Notations.** For the rest of the article, we will when needed denote

$$\limsup_{t \rightarrow +\infty} g(t) = \overline{\lim}_{t \rightarrow +\infty} g(t), \quad \liminf_{t \rightarrow +\infty} g(t) = \underline{\lim}_{t \rightarrow +\infty} g(t), \quad (4.14)$$

For a continuous real-valued function  $f$  defined on a compact set, we denote  $f^m$  and  $f^M$  its minimum and maximum. Finally,  $\delta_x$  denotes the Dirac mass at the position  $x$ .

#### 4.1.1 Asymptotics for tumour cells alone

In the absence of immune response (for instance, assuming either that there are no competent immune cells initially, i.e.,  $\ell^0 = 0$ , or that immune cells are inefficient in interacting with cancer cells through either  $\psi = 0$  or  $\mu = 0$ ), the first equation of (4.10) boils down to a standard logistic integro-differential model, namely

$$\begin{cases} \frac{\partial n}{\partial t}(t, x) = [r(x) - d(x)\rho(t)]n(t, x), & n(t = 0, x) = n^0(x) \geq 0, \\ \rho(t) = \int_0^1 n(t, x)dx. \end{cases} \quad (4.15)$$

The asymptotic behaviour of this equation is well known [16, 14, 18]. For any positive continuous initial condition  $n^0$ , the total population of tumour cells  $\rho(t)$  converges to  $\rho^* := \max(\frac{r}{d})$  as  $t \rightarrow +\infty$ .

This asymptotic cell population number, which is its maximal value, is readily interpreted, as for all logistic models of tumour growth, as the tumour *carrying capacity*. Furthermore, the density  $n(t, \cdot)$  viewed as a Radon measure supported on  $[0, 1]$  concentrates on the set

$$A := \{x \in [0, 1], r(x) - d(x)\rho^* = 0\} = \arg \max_{x \in [0, 1]} \frac{r(x)}{d(x)} \quad (4.16)$$

as  $t \rightarrow +\infty$ . If  $A$  is reduced to a singleton  $x^*$ , then in particular  $n(t, \cdot) \rightarrow \rho^* \delta_{x^*}$  as  $t \rightarrow +\infty$  in  $\mathcal{M}([0, 1])$ .

#### 4.1.2 A priori bounds

We first indicate the derivation of an upper bound for  $\rho$ . Integrating the first equation of system (4.10) with respect to  $x$ , we find using  $\varphi \geq 0$ :

$$\frac{d\rho}{dt} = \int_0^1 [r(x) - d(x)\rho - \mu(x)\varphi(t)]n(t, x)dx \leq \max_{x \in [0, 1]} (r(x) - d(x)\rho)\rho.$$

The right-hand side is negative as soon as  $\max_{x \in [0, 1]} (r(x) - d(x)\rho) < 0$ , i.e., as soon as  $\rho > \max \frac{r}{d}$ . Hence

$$\rho(t) \leq \rho^M =: \max \left( \rho(0), \max_{x \in [0, 1]} \frac{r(x)}{d(x)} \right), \quad \forall t > 0. \quad (4.17)$$

Consequently, we have

$$\forall y \in [0, 1], \quad \chi(t, y) \leq \omega^M \rho^M \quad \forall t \in [0, +\infty). \quad (4.18)$$

Let us fix  $y \in [0, 1]$ . From the bounds (4.17) and (4.18), we have

$$\frac{d}{dt} p(t, y) \leq [\omega^M \rho^M - k_2 p(t, y)] p(t, y). \quad (4.19)$$

By the comparison principle, we find

$$p(t, y) \leq p^M(y) := \max \left( p^0(y), \frac{\omega^M \rho^M}{k_2} \right), \quad \forall t > 0. \quad (4.20)$$

Using the same arguments, one can prove that the population density  $\ell$  is bounded from above. Indeed,

$$\frac{d}{dt} \ell(t, y) = p(t, y) - (\nu(y)\rho(t) - k_1) \ell(t, y) \leq p(t, y) - k_1 \ell(t, y) \leq p^M(y) - k_1 \ell(t, y). \quad (4.21)$$

Applying the comparison principle, we have

$$\ell(t, y) \leq \ell^M(y) := \max \left( \ell^0(y), \frac{p^M(y)}{k_1} \right), \quad \forall t > 0. \quad (4.22)$$

As a result, we obtain

$$\varphi(t) \leq \varphi^M := \int_0^1 \psi(y) \ell^M(y) dy, \quad \forall t > 0. \quad (4.23)$$

Finally, we may argue as above for a lower bound for  $\rho$  (on top of nonnegativity  $\rho \geq 0$ ). Indeed, from

$$\frac{d\rho}{dt} \geq \min_{x \in [0, 1]} (r(x) - d(x)\rho - \mu(x)\varphi^M) \rho, \quad (4.24)$$

it follows that

$$\rho(t) \geq \rho^m := \min \left( \rho(0), \min_{x \in [0, 1]} \left( \frac{r(x) - \mu(x)\varphi^M}{d(x)} \right) \right), \quad \forall t > 0. \quad (4.25)$$

We accordingly consider an assumption ensuring non-extinction, given by

$$\min_{x \in [0, 1]} \left( \frac{r(x) - \mu(x)\varphi^M}{d(x)} \right) > 0 \quad (4.26)$$

### 4.1.3 Asymptotics for the complete model, non-adaptive immune response case

This section is devoted to analysing the asymptotic behaviour of the model (4.10) in the non-adaptive case, particularly represented by NK-lymphocytes rather than by T-lymphocytes, where  $\varphi$  does not depend on  $x$ .

As already mentioned in Section 3, assuming all functions to be constant, the IDE system has the ODE (2) as a particular case. For that ODE, it has been proved that all three behaviours can occur: convergence to a (unique) trivial stable point (extinction or escape), convergence to a (unique) non-trivial stable point (equilibrium) and convergence to a limit cycle. The existence of such periodic solutions means that there is no hope of deriving any unconditional result of convergence to steady states for the IDE model.

In what follows, we prove a partial result, which makes the strong *a priori* assumption that  $n$  converges. Then we prove that the limit either equals 0 or can precisely be characterised, see Theorem 4.1.

**Proposition 4.1.** *Suppose that the density  $n$  weakly converges in  $\mathcal{M}([0, 1])$ , and denote  $n^\infty$  the limit measure. Setting  $\rho^\infty := \int_0^1 dn^\infty(x)$ , and under the assumptions (4.12)- (4.13), both densities  $\ell$  and  $p$  converge respectively to  $\ell^\infty, p^\infty \in C^0([0, 1])$  given by*

$$\begin{aligned}\ell^\infty(y) &= \frac{p^\infty(y)}{\nu(y)\rho^\infty + k_1}, \\ p^\infty(y) &= \frac{1}{k_2} \int_0^1 \omega(x, y) dn^\infty(x).\end{aligned}\tag{4.27}$$

*Proof.* We let  $y \in [0, 1]$  be fixed. First remark that  $\chi(t, y)$  converges to  $\bar{\chi}(y)$  given by

$$\bar{\chi}(y) := \int_0^1 \omega(x, y) dn^\infty(x).\tag{4.28}$$

Hence  $p(\cdot, y)$  satisfies a non-autonomous logistic ODE, given by

$$\frac{dp(t, y)}{dt} = [\chi(t, y) - k_2 p(t, y)] p(t, y).\tag{4.29}$$

For a given  $\varepsilon > 0$  and  $t$  large enough (say  $t \geq t_0$ ) such that  $\chi(t, y) \leq \bar{\chi}(y) + \varepsilon$ , we can write

$$\frac{dp(t, y)}{dt} \leq [\bar{\chi}(y) + \varepsilon - k_2 p(t, y)] p(t, y),\tag{4.30}$$

$p$  is thus a sub-solution of the equation

$$\frac{du}{dt}(t) = [\bar{\chi}(y) + \varepsilon - k_2 u(t)] u(t),\tag{4.31}$$

with initial condition chosen to be  $u(t_0) = p(t_0, y)$ . The solution of the latter logistic autonomous equation converges to  $\frac{\bar{\chi}(y) + \varepsilon}{k_2}$  as  $t \rightarrow +\infty$ , since  $p(t_0, y) > 0$  by the assumption (4.12). We conclude by the comparison principle that

$$\forall \varepsilon > 0, \quad \overline{\lim}_{t \rightarrow +\infty} p(t, y) \leq \lim_{t \rightarrow +\infty} u(t) = \frac{\bar{\chi}(y) + \varepsilon}{k_2}.\tag{4.32}$$

Therefore, we may pass to the limit  $\varepsilon \rightarrow 0$  in inequality (4.32) to obtain

$$\overline{\lim}_{t \rightarrow +\infty} p(t, y) \leq \frac{\bar{\chi}(y)}{k_2}.\tag{4.33}$$

Using the same reasoning from below, we have proved

$$\forall y \in [0, 1], \quad \lim_{t \rightarrow +\infty} p(t, y) = \frac{\bar{\chi}(y)}{k_2} = \frac{1}{k_2} \int_0^1 \omega(x, y) dn^\infty(x) = p^\infty(y).\tag{4.34}$$

Turning to the limit for  $\ell$ , we fix  $y$  in  $[0, 1]$ . Letting  $L_y(t) := l(t, y)$ , we have

$$\frac{dL_y(t)}{dt} = A_y(t) - B_y(t)L_y(t),\tag{4.35}$$

which is a non-autonomous linear differential equation, with

$$\begin{cases} \lim_{t \rightarrow +\infty} A_y(t) = \lim_{t \rightarrow +\infty} p(t, y) = p^\infty(y) =: \bar{A}_y, \\ \lim_{t \rightarrow +\infty} (\nu(y)\rho(t) + k_1) = \nu(y)\rho^\infty + k_1 =: \bar{B}_y. \end{cases}\tag{4.36}$$

For  $\varepsilon > 0$  small enough and  $t$  large enough (say  $t \geq t_0$ ) such that  $A_y(t) \leq \bar{A}_y + \varepsilon$  and  $B_y(t) \geq \bar{B}_y - \varepsilon$ , we can write

$$\frac{dL_y}{dt} \leq (\bar{A}_y + \varepsilon) - (\bar{B}_y - \varepsilon) L_y,\tag{4.37}$$

$L_y$  is thus a sub-solution of the autonomous equation given by

$$\frac{dv}{dt} = (\bar{A}_y + \varepsilon) - (\bar{B}_y - \varepsilon)v, \quad (4.38)$$

with  $v(t_0) = L_y(t_0)$ , the comparison principle allows us to conclude that

$$\forall \varepsilon > 0, \quad \overline{\lim}_{t \rightarrow +\infty} L_y(t) \leq \lim_{t \rightarrow +\infty} v(t) = \frac{\bar{A}_y + \varepsilon}{\bar{B}_y - \varepsilon}. \quad (4.39)$$

We then let  $\varepsilon$  go to 0 to get

$$\forall y \in [0, 1], \quad \overline{\lim}_{t \rightarrow +\infty} L_y(t) \leq \frac{\bar{A}_y}{\bar{B}_y} = \frac{p^\infty(y)}{\nu(y)\rho^\infty + k_1}. \quad (4.40)$$

Arguing in a similar manner to get a lower bound, we find

$$\forall y \in [0, 1], \quad \lim_{t \rightarrow +\infty} \ell(t, y) = \frac{p^\infty(y)}{k_1 + \nu(y)\rho^\infty} = \ell^\infty(y). \quad (4.41)$$

□

Let us now explain how to determine possible limits for the system, still making the strong *a priori* assumption that  $n(t, \cdot)$  converges. We shall need a technical (but rather weak) assumption, namely

$$\forall \bar{\rho} > 0, \forall \bar{\varphi} > 0, \quad \arg \max_{x \in [0, 1]} (r(x) - d(x)\bar{\rho} - \mu(x)\bar{\varphi}) =: \{x(\bar{\rho}, \bar{\varphi})\}. \quad (4.42)$$

From the proof and by the *a priori* bounds, one can see that this can be weakened by restricting the above assumption to the values  $0 < \bar{\rho} \leq \rho^M$ ,  $0 < \bar{\varphi} \leq \varphi^M$  such that the function  $x \mapsto r(x) - d(x)\bar{\rho} - \mu(x)\bar{\varphi}$  has maximum zero.

**Theorem 4.1.** *Suppose that the density  $n$  weakly converges in  $\mathcal{M}([0, 1])$ , and denote  $n^\infty$  the limit measure. Under the assumptions (4.12)-(4.13)-(4.42), then either  $n^\infty = 0$  or  $n^\infty$  is of the form*

$$n^\infty = \rho^\infty \delta_{x^\infty},$$

where  $x^\infty = x(\rho^\infty, \varphi^\infty)$  and  $(\rho^\infty, \varphi^\infty)$  solves the following system over  $(\rho, \varphi) \in \mathbb{R}^2$

$$\begin{cases} \rho = \max_{x \in [0, 1]} \left( \frac{r(x) - \mu(x)\varphi}{d(x)} \right), \\ \varphi = \frac{\rho}{k_2} \int_0^1 \frac{\psi(y)\omega(x(\rho, \varphi), y)}{\nu(y)\rho + k_1} dy. \end{cases} \quad (4.43)$$

**Remark 4.1.** *If one makes the additional assumption (4.26),  $\rho$  is bounded away from 0 and hence we must have  $n^\infty \neq 0$ . In other words, the only possible limits are of the form given by the above result if (4.26) holds.*

*Proof.* We assume that  $n^\infty \neq 0$ .

According to Proposition 4.1, both  $t \mapsto \ell(t, \cdot)$  and  $t \mapsto p(t, \cdot)$  converge pointwise to  $\ell^\infty$  and  $p^\infty$  implicitly given by formulae (4.27).

Let us justify that  $\varphi$  converges. The bound (4.22) shows that the function  $(t, y) \mapsto \psi(y)\ell(t, y)$  is dominated by the continuous function  $y \mapsto \psi(y)\ell^M(y)$ , hence by the dominated convergence theorem, we have

$$\lim_{t \rightarrow +\infty} \varphi(t) = \varphi^\infty := \int_0^1 \psi(y)\ell^\infty(y) dy = \frac{1}{k_2} \int_0^1 \left[ \frac{\psi(y)}{\nu(y)\rho^\infty + k_1} \int_0^1 \omega(x, y) dn^\infty(x) \right] dy. \quad (4.44)$$

The asymptotic behaviour of  $n$  is exponential, governed by  $r(x) - d(x)\rho^\infty - \mu(x)\varphi^\infty$ , a quantity whose sign we now analyse.

- If  $r(x_0) - d(x_0)\rho^\infty - \mu(x_0)\varphi^\infty > 0$  for some  $x_0 \in [0, 1]$ , then there exists  $\varepsilon > 0$  such that by continuity  $r - d\rho - \mu\varphi > \varepsilon$  on some open interval  $I \subset [0, 1]$  containing  $x_0$ , and all  $t$  large enough (say  $t \geq t_0$ ). As a result, for all  $t \geq t_0$ ,

$$\rho(t) = \int_0^1 n(t, x) dx \geq \int_I n(t_0, x) \exp^{\int_{t_0}^t (r(x) - d(x)\rho(s) - \mu(x)\varphi(s)) ds} dx \geq |I| \inf_{x \in I} n(t_0, x) \exp^{\varepsilon(t-t_0)}.$$

with  $|I|$  the length of  $I$ . Recalling the assumption (4.12), the continuous function  $n(t_0, \cdot)$  is also positive, which shows that  $\inf_{x \in I} n(t_0, x) > 0$ . Since the right-hand side goes to  $+\infty$ , we obtain a contradiction with the convergence of  $\rho$ .

- If  $r - d\rho^\infty - \mu\varphi^\infty < 0$  on the whole of  $[0, 1]$ , then using similar arguments, one can prove that  $\rho$  converges to 0 which is incompatible with the convergence of  $\rho$  to a positive limit (since  $n^\infty \neq 0$ ).

The function  $r - d\rho^\infty - \mu\varphi^\infty$  is thus non positive on  $[0, 1]$ , and its maximum equals 0. This is equivalent to saying that  $\rho^\infty = \max(\frac{r - \mu\varphi^\infty}{d})$ .

Assumption (4.42) ensures that the maximum point  $x^\infty := x(\rho^\infty, \varphi^\infty)$  is unique. Furthermore, the first bullet further shows that  $n(t, x)$  vanishes at any other point  $x$  than  $x \neq x^\infty$ . We have thus proved that  $n$  concentrates at  $x^\infty$ , hence  $n^\infty = \rho^\infty \delta_{x^\infty}$ .

Finally, inserting  $n^\infty = \rho^\infty \delta_{x^\infty}$  into the formula (4.44), we obtain the second equation, concluding the proof.

**Remark 4.2.** *In general, there is no close formula for the solutions of (4.43), which may not be unique. In practice, this system is easily solved numerically, for instance by a fixed point method. Hence, assuming convergence of  $n$ , this theorem does provide a rather complete picture of the possible non-trivial limits the system may reach. When there exists a unique solution to (4.43), a single such limit is hence characterised.*

□

#### 4.1.4 Asymptotics in the adaptive case

We now sketch the extension of Theorem 4.1 to the (more general) case where  $\varphi$  depends on  $x$ . In this case, we may obtain a result similar to Theorem 4.1, but at the expense of an assumption stronger than (4.42) and a more intricate system solved by the stationary state.

Indeed, keeping the same notations, we make the assumption that for all  $0 < \bar{\rho} \leq \rho^M$  and for all functions  $\bar{\ell} \in \mathcal{C}([0, 1])$  satisfying  $0 \leq \bar{\ell}(y) \leq \ell^M(y)$ ,

$$\arg \max_{x \in [0, 1]} \left( r(x) - d(x)\bar{\rho} - \mu(x) \int_0^1 \psi(x, y) \bar{\ell}(y) dy \right) =: \{x(\bar{\rho}, \bar{\ell})\}. \quad (4.45)$$

Following the proof of Theorem 4.1, one can then prove in exactly the same way:

**Theorem 4.2.** *Under the assumptions (4.12)-(4.13)-(4.45), supposing that  $n$  converges weakly in  $\mathcal{M}([0, 1])$  to some  $n^\infty$ , then either  $n^\infty = 0$  or  $n^\infty$  is of the form*

$$n^\infty = \rho^\infty \delta_{x^\infty},$$

where  $x^\infty = x(\rho^\infty, \ell^\infty)$  and  $(\rho^\infty, \ell^\infty)$  solves the following system over  $(\rho, \ell) \in \mathbb{R} \times \mathcal{C}([0, 1])$

$$\begin{cases} \rho = \max_{x \in [0, 1]} \left( \frac{r(x) - \mu(x) \int_0^1 \psi(x, y) \ell(y) dy}{d(x)} \right), \\ \ell(y) = \frac{\rho \omega(x(\rho, \ell), y)}{k_2 \nu(y)\rho + k_1}. \end{cases} \quad (4.46)$$

## 5 Numerical simulations

### 5.1 Simulations in the absence of treatment

In this section, we present some numerical simulations of system (4.10). The simulations are performed in Matlab using the parameters listed in Table 1, which have been chosen arbitrarily in the absence of suitable experimental data, in order to reproduce different biological scenarios. We follow the numerical method given in [19] and we select a discretisation of the phenotype interval  $[0, 1]$  consisting of 1000 points for the computational domain of the independent variables  $x$  and  $y$  and let  $t \in [0, T]$ , unless otherwise specified, we choose the final time  $T = 1000$ .

To define the initial density of tumour cells, we use a Gaussian profile, and a homogeneous condition for competent immune cells  $\ell$ , while the naive immune cells  $p$  are distributed over the whole interval  $[0, 1]$ :

$$\begin{cases} n^0(x) = n(0, x) = \frac{C}{\sqrt{2\pi\sigma_0^2}} \exp\left(\frac{-(x-m)^2}{2e^2}\right), \\ \ell^0(y) = \ell(0, y) = 0, \\ p^0(y) = p(0, y) = 1 - y^2, \end{cases} \quad (5.47)$$

with  $m = 0.5, e = 0.1$ , and a normalisation constant  $C > 0$  chosen so that  $\rho(0) = 1$ . Thus, we start with a total mass equal to 1, and the phenotype  $x$  is initially concentrated at 0.5.

**Remark 5.1.** • *For simulations illustrated on Figures 4-6, 8-10, and 11-12: **Upper row.** Evolution in time of the normalised densities  $x \mapsto \frac{n(t,x)}{\rho(t)}$  (left panel);  $y \mapsto \frac{\ell(t,y)}{\sigma(t)}$  (central panel), and  $y \mapsto \frac{p(t,y)}{\gamma(t)}$  (right panel), with the initial conditions in blue, and the final ones in red. **Lower row.** Dynamics of the total number of tumour cells  $\rho(t)$  (left panel); dynamics of the total number of competent immune cells  $\sigma(t)$  (central panel); dynamics of the total number of naive immune cells  $\gamma(t)$  (right panel).*

- *We will assume that the competent T-cells  $\ell(t, y)$  are absent at time  $t = 0$  and that the most aggressive naive T-cells  $p(t, y)$  have been duly informed by APCs and are already present at the tumour site.*
- *We explore both types of the anti-tumour immune response characterised by different forms of the function  $\varphi$ .*

Parameter/function	Biological meaning	Value
$r(x)$	Proliferation rate of tumour cells	$0.666 - 0.132x^2$
$d(x)$	Death rate of tumour cells	$0.5(1 - 0.3x)$
$\mu(x)$	Sensitivity to the effects of the immune response	$1 - 0.1x^2$
$\psi(y)$	Efficacy of the immune response	$0.5y^2$
$\nu(y)$	Immunotolerance of immune cells induced by tumour cells	$0.5 - 0.1y$
$k_1$	Natural death rate of competent immune cells	0.5
$k_2$	Carrying capacity of naive immune cells	1.5
$\alpha$	Strength of the immune response	1

Table 1: Values of the model parameters/functions used to carry out numerical simulations.

**Tumour development in the absence of the immune response.** We begin by establishing a baseline scenario in which tumour cells proliferate and die according to the modelling approach described in Section 3, i.e., in the absence of the immune response, the growth of the tumour cell population is of the logistic type.

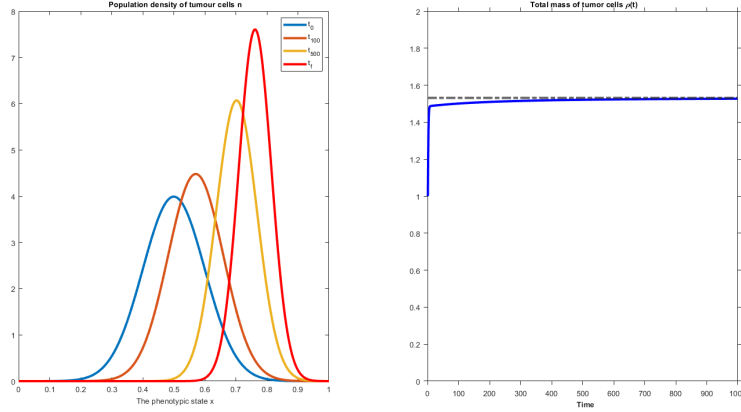


Figure 3: **Numerical simulation of the solution to (4.15)** (complete absence of immune response). **Left panel**, plots of cell densities  $n(t, \cdot)$  at different times up to  $T = t_f = 1000$  (in red): the phenotype  $x$  evolves towards more and more malignancy. **Right panel**, dynamics of the total density of tumour cells  $\rho(t)$ . The black dashed line highlights a numerical estimation of the tumour cell carrying capacity  $\rho^*$  and the parameter values are as listed on Table 1, with  $\rho(0) = 1$ .

According to Section 4, we expect convergence of  $\rho$  and weak convergence of  $n$  to a weighted Dirac mass at  $x^* \approx 0.8587$  in  $\mathcal{M}([0, 1])$ , which is indeed the case illustrated on Figure 3. Moreover, the limit for  $\rho$  is  $\rho^* = \max(\frac{r}{d})$ , which corresponds to the carrying capacity of the tumour, i.e., the saturation term reached by the total number of tumour cells due to within-population competition for space and resources. Here,  $\rho^* \approx 1.5320$  and this is what we observe numerically on Figure 3 to the right.

As already mentioned in the introduction, we will from now on, when the immune response is activated, interpret solutions for which the total number of tumour cells approaches this carrying capacity  $\rho^*$  as “tumour escape”. This represents one case of the three  $E$ s in which the immune cells are present at the tumour site but are inefficient in interacting with the tumour cells.

### 5.1.1 Simulations for the innate-immune response case

In the following subsection, we present numerical results for the *innate* (non-specific) anti-tumour immune response ( $\varphi = \varphi(t)$ ), assumed to be due to the killing action on the tumour site of NK-lymphocytes, that have been activated in tissues and lymphoid organs by messages from circulating NK-cells. Each simulation is carried out by keeping all parameter values fixed as in Table 1, and taking three different choices of the parameter  $s$ , which is a measure of the precision of the localisation of the phenotype  $x$  with respect to the phenotype  $y$  at the tumour site: the smaller  $s$  is, the sharper the precision.

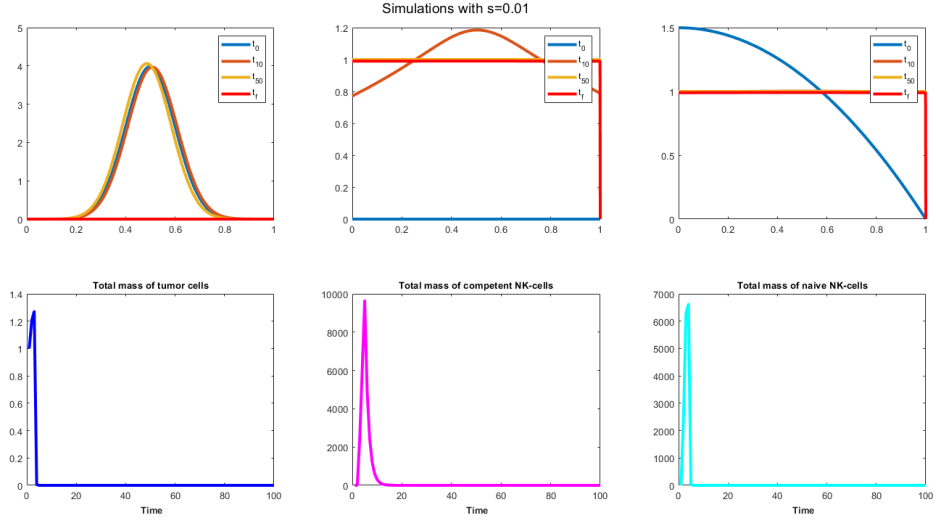


Figure 4: **Eradiation.** Simulations with  $s = 0.01$  for  $T = 100$ , using the parameter values listed in Table 1 and the values of the initial conditions  $n^0(x), \ell^0(y), p^0(y)$  given in equation (5.47). The population of tumour cells is Gaussian-shaped, decreasing exponentially to 0, which means that the immune response becomes very effective and leads to the total eradication of tumour cells. Moreover, the phenotypic distribution of the tumour cells population remains unimodal throughout the entire time, with the mean phenotypic state being at the initial point of the distribution, while, both populations of NK cells are uniformly distributed over  $[0, 1]$ .

We also mention that, when the parameter  $s$  is small enough, the assumption (4.26) is no longer satisfied. Depending on the parameters and without this assumption, we may have  $\rho(t) \rightarrow 0$  or convergence to a positive value. In the former case  $\rho(t) \rightarrow 0$ , no control with *ICIs* would be necessary.

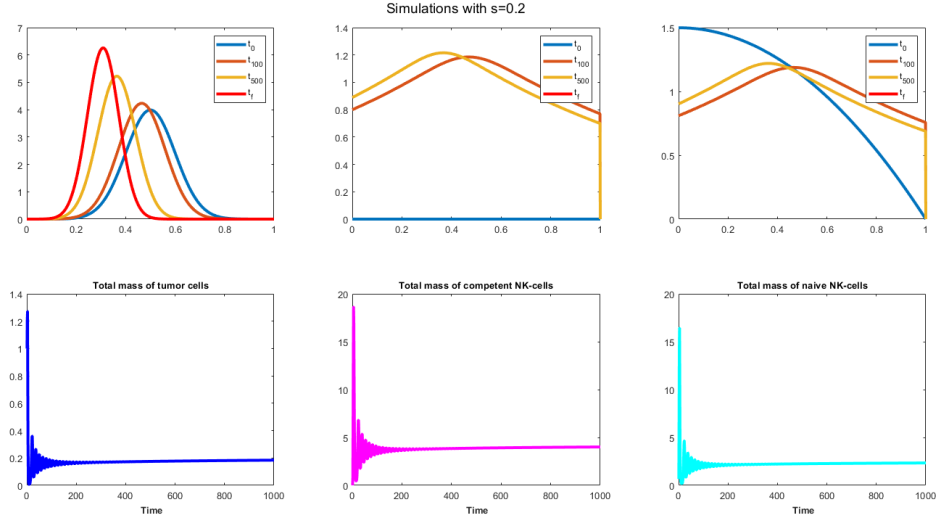


Figure 5: **Equilibrium.** Simulations with  $s = 0.2$  for  $T = 1000$ , and all the other parameters and functions are as in Table 1. When the parameter  $s$  is large enough so that the condition (4.26) is satisfied, the total density of tumour cells decreases over time until it reaches a relatively small value. In the meantime, the population of tumour cells becomes less malignant (upper left panel).

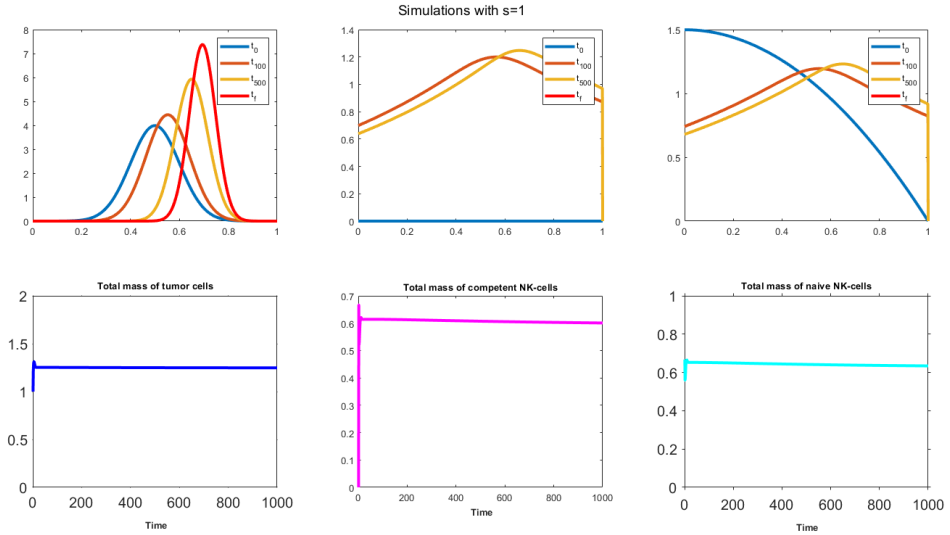


Figure 6: **Escape.** Simulations with  $s = 1$  for  $T = 1000$ . The total number of tumour cells overtakes the total number of CD8+ T cells and keeps growing until saturation. The asymptotic total number of tumour cells is found to be very slightly below the carrying capacity  $\rho^* = \max(\frac{r}{d})$ , in agreement with formula (4.43) for a relatively small value of  $\varphi^\infty$ . The malignancy phenotype  $x$  is on the increase (upper left panel).

According to what is expected from Theorem 4.1, the numerical results displayed in Figure 5 show that the tumour cell population  $n(t, x)$  becomes concentrated as a Dirac mass centred at the point  $x^\infty \approx 0.31$ : it means that tumour cells become less and less malignant as time goes by. Both total

densities  $(\rho(t), \varphi(t))$  converge to their asymptotic values given by (4.43), which are numerically equal to  $(\rho^\infty, \varphi^\infty) \approx (0.1873, 0.5750)$  (see figure 7, middle panel). Of note, the equilibrium situation can be recovered by taking  $0 < s < 1$  large enough. As  $s$  increases, the equilibrium is reached faster, with less oscillations but it leads to an asymptotic state with a larger tumour mass, which is its apparent carrying (maximum) capacity, representing the “escape” state of the three  $E$ s of immunoediting (see Figure 6). Let us also mention that there is a perfect match between the asymptotic values given by Theorem 4.1 and the ones obtained numerically.

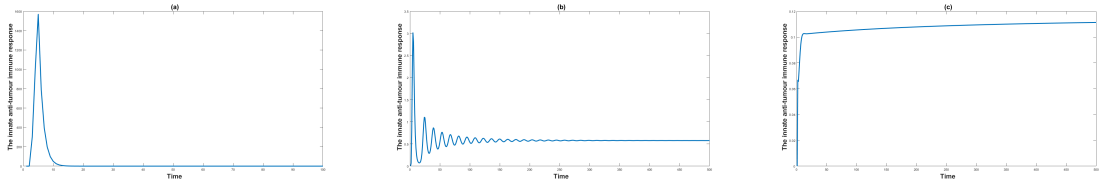


Figure 7: **Graphs of  $t \mapsto \varphi(t)$ : immune response mediated by NK-cells corresponding respectively to simulations of Figures 4-6.** Three values of the parameter  $s$  are tested: **a,c**  $s = 0.01$ ,  $s = 0.2$ , and  $s = 1$  and all other values are reported in Table 1. Here the final time is  $T = 100$  for plot in panel (a) and  $T = 500$  for plots in panels (b)-(c).

As shown in Figure 7 in panels (b)-(c), the function  $\varphi(t)$  increases or oscillates until it reaches a maximum plateau; on the other hand,  $\varphi(t)$  increases in a faster way, and it does not reach a plateau but directly decreases to 0 in panel (a) for a small value of  $s$ .

### 5.1.2 Simulations for the adaptive (specific) case

In the sequel, we keep the same model and data as in Table 1, but we deal with the adaptive specific anti-tumour immune response ( $\varphi = \varphi(t, x)$ ), assumed to be related to the action on tumour cells of CD8+ T lymphocytes, that have been activated in lymphoid organs by APCs. We investigate the way in which the outcomes of the simulations are affected by key parameters whose impacts on the dynamics of tumour cells and T cells are biologically relevant. Such key parameters are the specificity  $s$  of the message transmitted by APCs to the lymphoid organs, and the specificity  $v$  of the anti-tumour immune response. Moreover, having in mind to explore, further, than the strictly adaptive case in which  $\varphi = \varphi(t, x)$ , a mixed case representing both the non-adaptive activation (by sensing lacking MHC-I antigens on tumour cells) of the innate immune response ( $\varphi = \varphi(t)$ ) by patrolling NK-lymphocytes, and the activation by APCs of the adaptive specific immune response ( $\varphi = \varphi(t, x)$ ) by CD8+ T-cells, we will in the sequel also consider a convex combination of the two responses, of the form:

$$\varphi(t, x) = \int_0^1 \Psi(x, y) \ell(t, y) dy, \quad (5.48)$$

where the function  $\Psi$  is the following convex combination of the two cases

$$\Psi(x, y) = \left( 1 - \lambda + \frac{\lambda}{v} e^{-|x-y|/v} \right) \psi(y), \quad \lambda \in [0, 1], \quad (5.49)$$

with the aim to consider the two extreme cases, innate and strictly adaptive, together with a non-trivial convex combination of them. In this representation:

- $\lambda = 0$  corresponds to the *innate non-adaptive* anti-tumour immune response, already explored in section 5.1.1, and analysed in section 4.1.3;
- $\lambda = 1$  corresponds to the *strictly adaptive* anti-tumour immune response;
- $0 < \lambda < 1$  corresponds to cases for which both anti-tumour immune responses are active.

Note that such a convex combination is a simplified representation of the actual immune response, as we consider the two responses to be independent of one another, which is likely to not be the case of a real immune response.

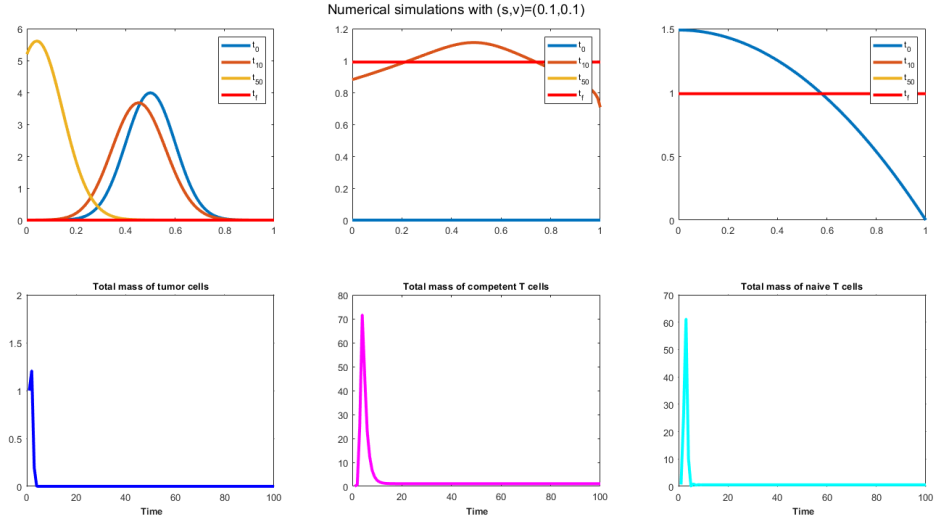


Figure 8: **Eradiation.** Strictly adaptive case ( $\lambda = 1$ ). Simulations with  $(s, v) = (0.1, 0.1)$  for  $T = 100$ .

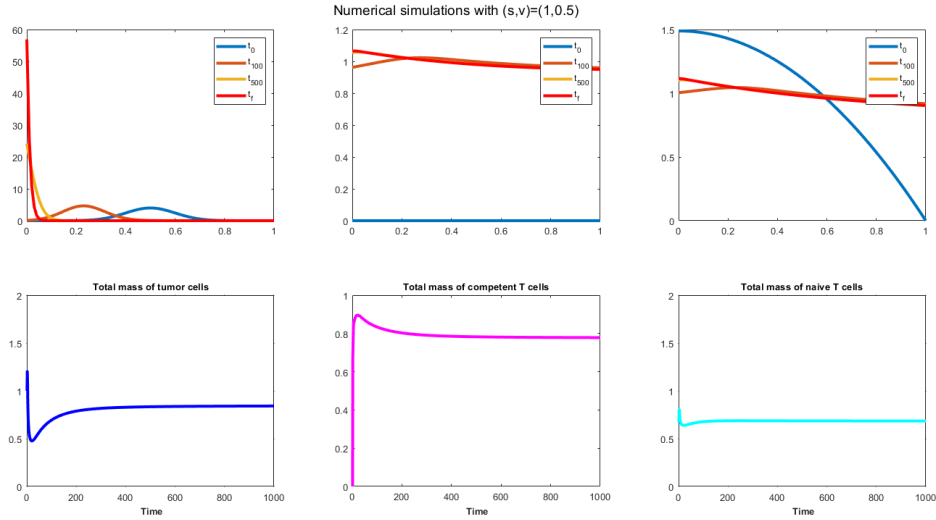


Figure 9: **Equilibrium.** Strictly adaptive case ( $\lambda = 1$ ). Simulations with  $(s, v) = (1, 0.5)$  for  $T = 1000$ .

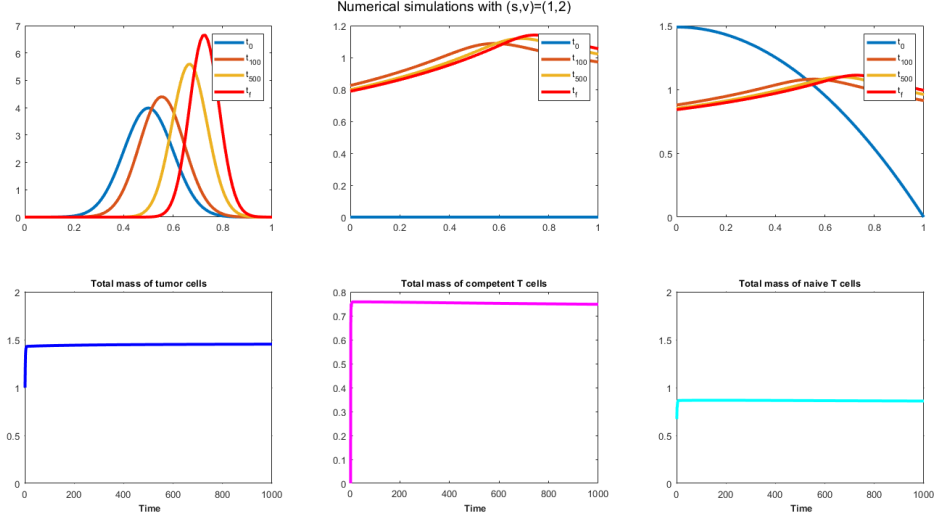


Figure 10: **Escape.** Strictly adaptive case ( $\lambda = 1$ ). Simulations with  $(s, v) = (1, 2)$  for  $T = 1000$ .

When the parameter  $s$  is small enough, and for all considered values of the parameter  $v$ , the total number of tumour cells decreases steadily over time until the tumour cell population is completely eradicated (Figure 8). This is due to the fact that in the case of the strictly adaptive response, good transmission of the malignancy phenotype  $x$  by APCs (i.e., small values of the parameter  $s$  in the function  $\chi(t, y)$ ) promotes the eradication of tumour cells by CD8+ T-lymphocytes cells. The results displayed on Figure 9 show that intermediate values of the parameter  $s$  and  $v$  facilitate the coexistence between tumour and immune CD8+ T-lymphocytes, while the total number of tumour cells remains at a low level. Finally, Figure 10 shows that under the choice of parameters in the computational simulations illustrated on Figure 9, increasing the value of the parameter  $v$  leads to tumour escape. These results suggest the idea that the efficiency of the anti-tumour immune response is affected by the specificity of the anti-tumour immune response and the specificity of the message transmitted by APCs to the naive T cells. In summary, increasing values of parameters  $s$  and  $v$  respectively is associated with low numbers of immune cells and less effective immune response which may benefit tumour development.

**Combination of both innate and adaptive anti-tumour immune responses** In this subsection, we present numerical simulations that incorporate the innate and adaptive immune response by taking an intermediate value of the parameter  $\lambda = 0.5$ , and we compare these results with those displayed in the previous paragraphs. We will numerically show how the outcomes of the tumour-immune response interactions change as we vary the specificity of the anti-tumour immune response  $v$  for a fixed value of  $s = 1$ . All the values of the other parameters and functions are as in Table 1.

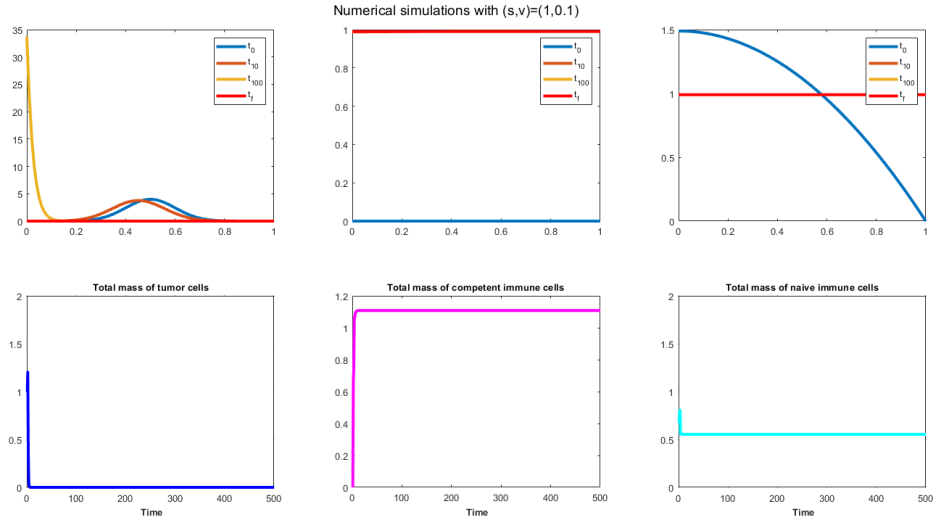


Figure 11: **Eradiation.** Mixed innate/adaptive case ( $\lambda = 0.5$ ). Simulations with  $(s, v) = (1, 0.1)$  for  $T = 500$ .

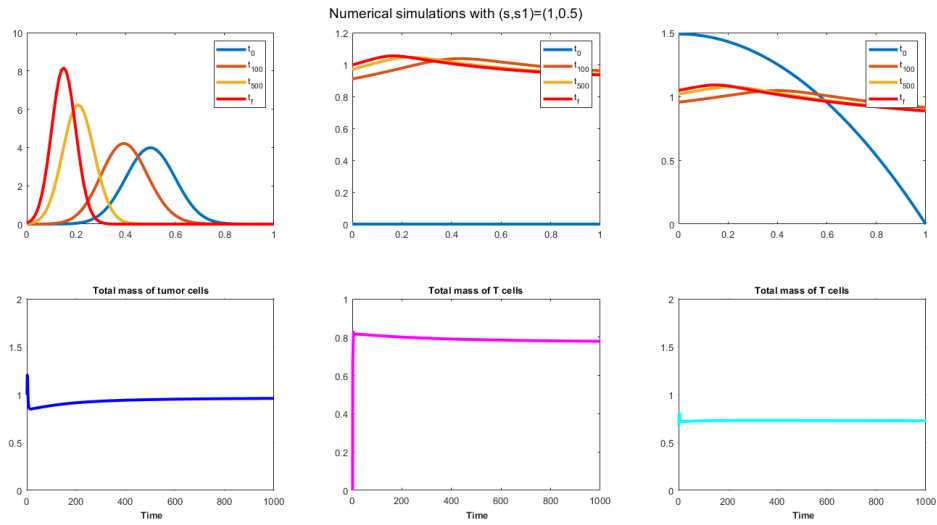


Figure 12: **Equilibrium.** Mixed innate/adaptive case ( $\lambda = 0.5$ ). Simulations with  $(s, v) = (1, 0.5)$  for  $T = 1000$ .

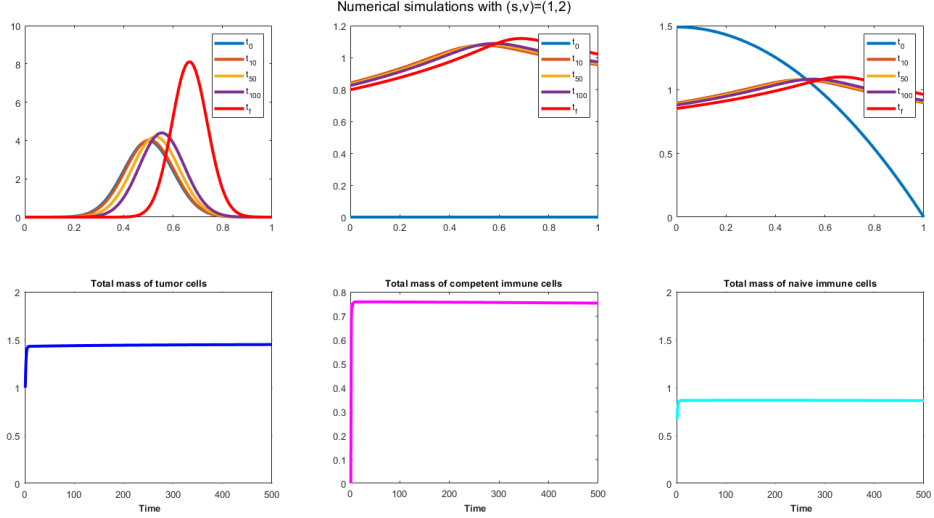


Figure 13: **Escape.** Mixed innate/adaptive case ( $\lambda = 0.5$ ). Simulations with  $(s, v) = (1, 1)$  for  $T = 1000$ .

As shown on Figures 11-13, for intermediate values of the parameter  $\lambda$  in  $[0, 1]$ , dynamics similar to those of a strictly adaptive anti-tumour immune response are observed numerically in the case of a mixed anti-tumour immune response. More precisely, for low values of the parameter  $v$ , the specific anti-tumour immune response involving CD8+ T-lymphocytes is relatively high, leading to the total eradication of tumour cells; intermediate values of  $v$  lead to a co-existence state representing tumour-immune response equilibrium; and finally, sufficiently high values of  $v$  decrease the efficiency of the specific immune response and lead to the emergence of malignant tumour cells.

Taken together, the numerical results that we have presented in the previous subsections suggest that the model has validity for providing a consistent qualitative description of the anti-tumour immune response involving both NK cells and CD8+ T-lymphocytes.

**Periodic solutions.** We now numerically address the existence of periodic solutions. We first take all the parameters and functions to be equal to those chosen for the ODE model in the periodic case, those used to obtain Figure 2. Then, we perturb them by a small parameter  $0 < \delta \ll 1$ . In this case, an oscillatory behaviour also emerges, corresponding to a co-existence state representing a time-dependent periodic solution, see Figure 14. We have not been able to analytically address the existence of periodic solutions, except for the very specific case where all functions are constant, in which case we recover 2, for which we know periodic solutions do exist [9].

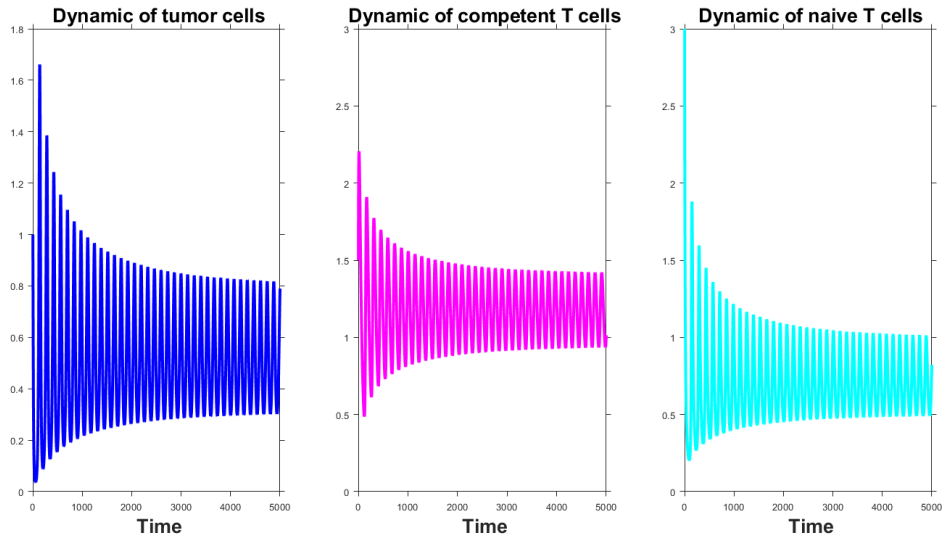


Figure 14: Evolution with time of the tumour total density  $\rho(t)$  (in blue), competent T cells total density  $\sigma(t)$  (in magenta), and the total density of naive T cells  $\gamma(t)$  (in cyan) for  $T = 5000$ .

## 5.2 Increasing *ICI*: from escape to equilibrium

The results presented in the previous subsections summarise how the three Es of immunoediting can occur under different combinations of values for the parameters  $s$  and  $v$ . We now explore the possible outcomes of immunotherapy with immune checkpoint inhibitors where only the adaptive anti-tumour immune response is active (i.e.,  $\lambda = 1$ ). This corresponds to a biological scenario in which an anti-PD1 immunotherapy is used to boost the exhausted T-cells.

As mentioned in section 4, we will present numerical simulations with constant (in time) control *ICI*. In particular, we placed ourselves in the same configuration as on Figure 10, a choice of parameters that resulted, with  $ICI = 0$ , in tumour escape. We numerically solve the same mathematical problem considered in the previous subsections taking now *ICI* to be constant over time, from  $ICI = 1$  to  $ICI = 10$ .

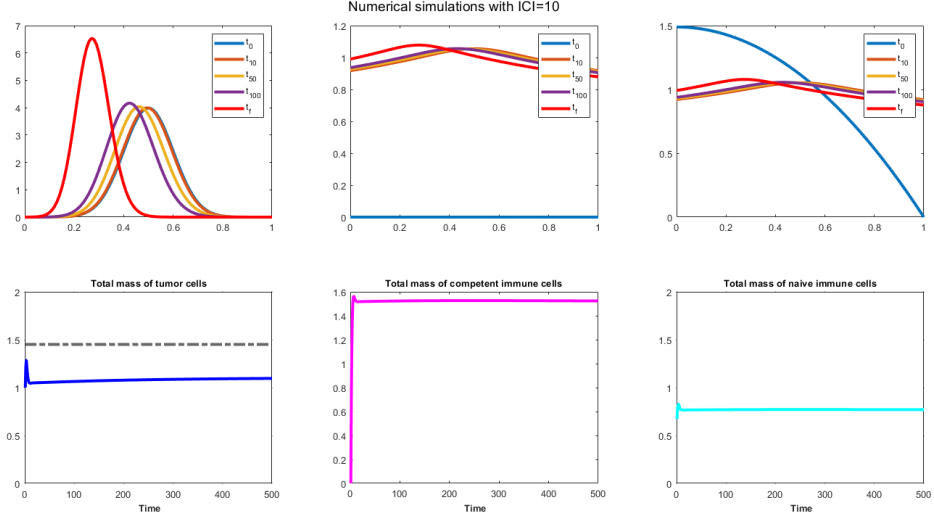


Figure 15: **Simulation with  $ICI = 10$  and  $h = 10$ , at time  $T = 500$ .** Simulations have been carried out using the parameter values listed in Table 1. The black dashed line highlights the total density  $\rho^*$  of tumour cells at the end of numerical simulation in the scenario “without treatment” (i.e.,  $ICI = 0$ ). Compare also with Figure 10.

**Controlling tumour growth with  $ICIs$ .** The numerical results shown on Figure 15 illustrate the impact of a constant control  $ICI = 10$ , which allows to maintain the total density of tumour cells  $\rho$  close to its initial value  $\rho(0)$ , whereas the population of tumour cells becomes concentrated as a Dirac mass centred at the point  $x^\infty \approx 0.28$ , corresponding to a less aggressive phenotype. Comparing these results with those displayed on Figure 10, we see that, in general, for the same values of parameters  $s$  and  $v$ , taking  $ICI = 10$  slightly increases the number of competent immune cells and reduces tumour growth, taking the tumour below its carrying capacity, which represents an “equilibrium” state among the three Es. However, one can note that the tumour is not eradicated (and this holds whatever the chosen level of  $ICI$ ).

### 5.3 Possible extinction with $ICIs$ with a different function $\nu$

This last unsatisfactory remark leads us to nevertheless illustrate how a slightly modified version of the same model can show a situation in which increasing the level of  $ICIs$  can bring the tumour from escape or equilibrium to extinction. We define a new version of the immunotolerance function  $\nu$  by

$$\nu(y) = 1 - 0.1y, \quad (5.50)$$

and set the parameter for the natural death rate of competent T cells to  $k_1 = 0.01$ , keeping the other parameters as in Table 1.

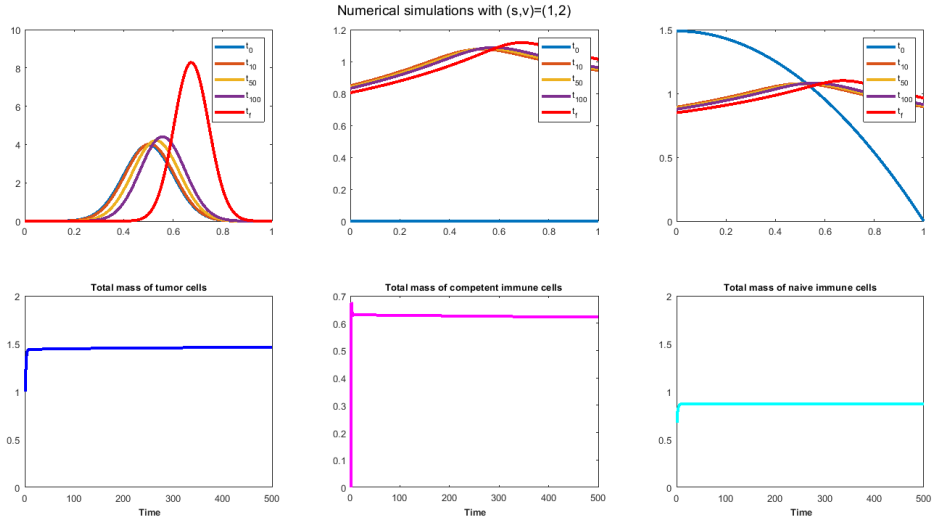


Figure 16: **Escape.** Simulation with  $ICI = 0$ , at time  $T = 500$ , with the new function  $\nu$  defined by 5.50, for the same simulation setup as of Figure 10 (strictly adaptive case). Here,  $k_1 = 0.01$ . As shown on the upper left panel, the malignancy phenotype level is high.

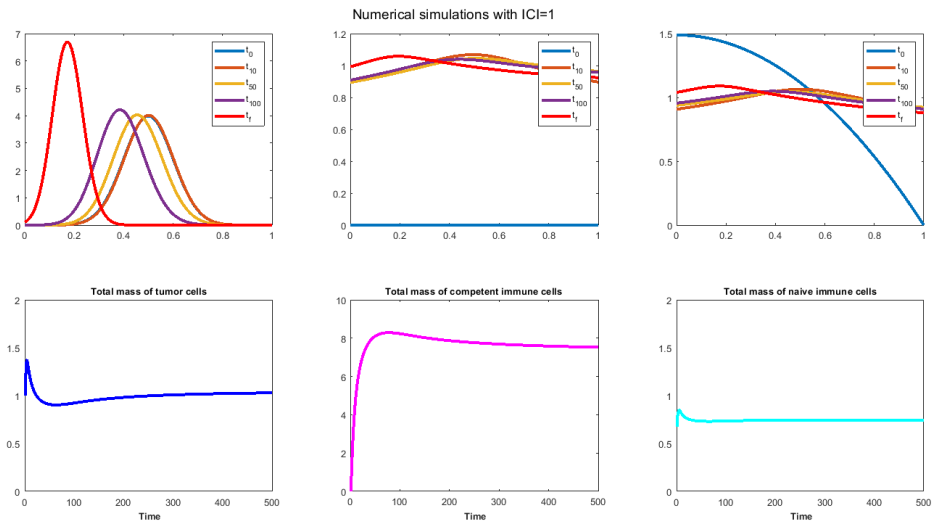


Figure 17: **Equilibrium.** Simulation with  $ICI = 1$  and  $h = 10$ , at time  $T = 500$ , with the new function  $\nu$  defined by 5.50 (strictly adaptive case). Here,  $k_1 = 0.01$ , and all the other parameters and functions are as in Table 1. Increasing the level of  $ICIs$  from 0 to 1 has led the tumour from escape to equilibrium. As shown on the upper left panel, the malignancy phenotype has notably decreased.

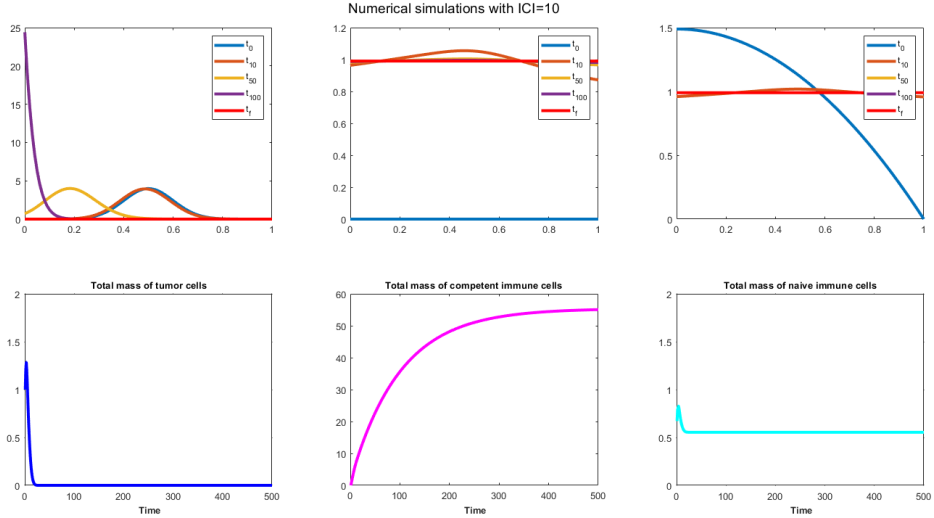


Figure 18: **Eradiation.** Simulation with  $ICI = 10$  and  $h = 10$ , at time  $T = 500$ , with the new function  $\nu$  defined by 5.50 (strictly adaptive case). Here,  $k_1 = 0.01$ , and all the other parameters and functions are as in Table 1. Increasing the level of  $ICIs$  to 10 has led the tumour from escape/equilibrium to eradication.

**Efficacy of the immune response.** With this new function, the simulation shown on Figure 15, with  $ICI = 10$  is completely modified, as can be seen on Figure 18, compared to Figures 16 and 17. Indeed, this time, the strategy consisting of taking a constant control with  $ICIs$  restores the immune efficacy and allows for the total eradication of tumour cells. These results also suggest that acting by  $ICIs$  to modify the immunotolerance function  $\nu$  in a different way, not only by just dividing its amplitude by means of the term  $1+hICI$ , and on  $k_1$ , may promote effective therapies with immune checkpoint inhibitors which affect the total density of tumour cells. Of course, one would then have to better define in some physiological way the immunotolerance function  $\nu$ , which is so far arbitrary. Such better, more physiological, definition would nonetheless require access to experimental measurements, which is presently beyond our reach.

## 6 Conclusions and research perspectives.

### 6.1 Summary of the mathematical results.

We have proposed a new mathematical model of tumour-immune interactions in which cell populations are structured by continuous phenotype variables representing their aggressiveness. Despite its simplicity, our model features some relevant phenomena, and it captures the three  $E$ s of immunoediting - eradication, equilibrium and escape. In particular, it reproduces the formation of an equilibrium, which characterises the capacity of the immune system to contain tumour growth.

In Section 4, we showed through an asymptotic analysis of the model that under the *a priori* assumption that the population of tumour cells converges to a certain measure, such a measure can precisely be characterised when it is not the trivial measure.

We explained why convergence cannot be the general outcome: our model does have the ODE system (2), with known possible periodic behaviour, as a particular case. Finding which parameters lead to convergence or to oscillatory behaviours is a completely open question.

Our model can incorporate three different types of anti-tumour immune responses: innate, adaptive, and a combination of both immune responses. By numerically comparing these three cases in Section 5, the outcomes are as follows:

**Innate anti-tumour immune response.** If the parameter  $s$ , which determines how localised the phenotype  $x$  is with respect to the phenotype  $y$ , is small enough, then the tumour is always eliminated. For intermediate values of  $s$ , we obtain convergence to a limit coherent with Theorem 4.1: a coexistence state occurs, yielding a persistent tumour cell population at a controlled level. Finally, high values of the parameter  $s$  reduce the efficiency of the anti-tumour immune response and lead to tumour escape. For particular choices of the model parameters, the numerical results also show periodic solutions, characterised by periodic alternating growth and decay of all the immune and tumour cell populations.

**Adaptive anti-tumour immune response.** The numerical results that we have presented demonstrate that within the adaptive anti-tumour response, both the specificity of the response of competent immune cells (i.e., the parameter  $v$ ) and the specificity of the message transmitted by APCs (i.e., the parameter  $s$ ) play a key role in the tumour-immune interactions. In fact, when  $s$  and  $v$  are both small, our results indicate that tumour eradication can occur, while higher values of  $s$  or  $v$  may result in tumour escape.

**Combination of the innate and the adaptive anti-tumour immune responses.** Increasing the specificity of the adaptive immune response (low values of the parameter  $v$ ) has a beneficial effect on the immune response to tumours, whereas higher values of the parameter  $v$  can be detrimental to the anti-tumour immune action.

**Simulations of the effect of constant drug doses.** The numerical simulations displayed in Section 5.2 show that a constant control allows to maintain the total density of tumour cells below its carrying capacity and prevents malignant tumour cells from taking over the whole population. We have also shown that slightly changing the immunotolerance rate along with the natural death rate of competent T cells improves the immune check-point inhibitor’s immunotherapy efficacy and that they can bring tumours from escape to eradication.

## 6.2 Biological interpretations.

Taking for granted the existence of a continuous malignancy trait in tumour cells, that we relate to a ‘degree of stemness’ or de-differentiation potential, and similarly, of a continuous potential of tumour cell-kill in lymphocytes at the contact of tumour cells, we have qualitatively produced scenarios that reproduce the three *Es* of immunoediting. We have shown that the initial malignancy trait of tumour cells is affected by the immune response, with or without boosting by *ICI* therapy, and that it will always concentrate on a pointwise value, meaning that tumour cells as a population organise their stemness trait around a fixed dominant characteristic. Whether this sharp malignancy trait is increased or decreased by the immune response cannot *a priori* be decided, as its determinants depend in a complex way on the entangled functions  $d$ ,  $r$ ,  $\mu$  and  $\varphi$  that govern the proliferation of the tumour cell population. If this model has some relevance with the reality of antitumoral immune response, it means that the effect of lymphocytes attacking a tumour may as well increase or decrease its stemness, which to the best of our knowledge is not inconsistent with biological observations so far. From a therapeutic point of view, we have shown, as proofs of concept, numerical case studies in which a tumour can be brought from escape to extinction, or at least equilibrium, by continuous delivery of *ICIs*.

## 6.3 Possible generalisations.

(i) Firstly, we plan to extend the model considered in this paper to carry out a mathematical study of tumour-response interactions, taking into account non-genetic instability, which may be considered as mediated by random epimutations in populations of tumour cells. In this respect, a modelling approach

analogous to the one presented in [12], would consist in modifying system 3.1 as follows:

$$\begin{cases} \frac{\partial n}{\partial t}(t, x) = [r(x) - d(x)\rho(t) - \mu(x)\varphi(t)] n(t, x) \left[ +\beta \frac{\partial^2 n}{\partial x^2}(t, x) \right], \\ \frac{\partial \ell}{\partial t}(t, y) = p(t, y) - (\nu(y)\rho(t) + k_1) \ell(t, y), \\ \frac{\partial p}{\partial t}(t, y) = \alpha\chi(t, y)p(t, y) - k_2 p^2(t, y). \end{cases} \quad (6.51)$$

The linear diffusion operator  $\beta \frac{\partial^2 n}{\partial x^2}(t, x)$ , with  $0 < \beta \ll 1$ , represents here a malignancy phenotype lability (uncertainty) linked to the extreme plasticity of cancer cells [23], that are able to vary their phenotype in response to any (drug or other environmental) insult.

(ii) Another natural way to extend our work would be to introduce a population of antigen-presenting cells (APCs), that recognises a tumour antigen as their cognate one to activate naive T-cells, instead of the time-independent shortcut function  $\omega(x, y)$  (see Section 3). Delays might also naturally be introduced in this bidirectional communication process.

(iii) Future research perspectives, from the point of view of confronting the model to data, are to identify its parameters, making use of preclinical and clinical data on the growth of in-vivo tumours in laboratory rodents and in melanoma patients exposed to *ICI* therapies. This, however, will necessarily rely on long-term collaborations with teams of laboratory experimentalists and clinicians, towards whom we have here only set this physiologically based model as a basis for interactive discussions to assess it qualitatively.

(iv) Finally, as exemplified in [18], it would be relevant to address numerical optimal control of model 3.1 in order to identify possibly optimal delivery schedules for the *ICI* therapies, which will also be intended in the framework of an interactive collaboration with experimentalists and clinicians.

## References

- [1] Abel, A.M., Yang, C., Thakar, M.S., Malarkannan, S. Natural Killer Cells: Development, Maturation, and Clinical Utilization. *Frontiers in Immunology*, 9:1869, 2018.
- [2] Almeida, L., Bagnerini, P., Fabrini, G., Hughes, B. D., Lorenzi, T. (2019). Evolution of cancer cell populations under cytotoxic therapy and treatment optimisation: insight from a phenotype-structured model. *ESAIM: Mathematical Modelling and Numerical Analysis*, 53(4), 1157-1190.
- [3] Alvarez, F.E., Carrillo, J.A., Clairambault, J. (2022). Evolution of a structured cell population endowed with plasticity of traits under constraints on and between the traits. *Journal of Mathematical Biology*, 85:64, published on line November 2022.
- [4] Bertolaso, M. (2016) *Philosophy of Cancer. A dynamic and relational view.* Springer Publisher.
- [5] Champagnat, N., Ferrière, R., Méléard, S. (2008). From individual stochastic processes to macroscopic models in adaptive evolution. *Stochastic Models*, 24(sup1), 2-44.
- [6] Clairambault, J., Pouchol, C. (2019). A survey of adaptive cell population dynamics models of emergence of drug resistance in cancer, and open questions about evolution and cancer. *BIOMATH*, vol. 8, issue 1, online May 2019 (23 pages).
- [7] Delitala, M., Lorenzi, T. (2013). Recognition and learning in a mathematical model for immune response against cancer. *Discrete and Continuous Dynamical Systems-B*, 18(4), 891.
- [8] Han, Y.Y., Liu, D.D., Li, L.H. (2020). PD-1/PD-L1 pathway: current researches in cancer, *American Journal of Cancer Research*, 10(3):727-742.
- [9] Kaid, Z., Lakmeche, A., Clairambault, J., Helal, M. (2022). Dynamics of tumor growth and of the immune response model. Submitted.

- [10] Lee, J.H., Shklovskaya, E., Lim, S.Y., Carlino, M.S., Menzies, A.M., Stewart, A., Pedersen, B., Irvine, M., Alavi, S., Yang, J.Y.H., Strbenac, D., Saw, R.P.M., Thompson, J.F., Wilmott, J.S., Scolyer, R.A., Long, G.V., Kefford, R.F., Rizos, H. (2020). Transcriptional downregulation of MHC class I and melanoma de- differentiation in resistance to PD-1 inhibition. *Nature Communications*, 11:1897.
- [11] Le Louedec, F., Leenhardt, F., Marin, C., Chatelut, É., Evrard, A., Ciccolini, J. (2020). Cancer Immunotherapy Dosing: A Pharmacokinetic/Pharmacodynamic Perspective. *Vaccines*, 8(4), 632.
- [12] Lorenzi, T., Chisholm, R. H., Clairambault, J. (2016). Tracking the evolution of cancer cell populations through the mathematical lens of phenotype-structured equations. *Biology direct*, 11(1), 1-17.
- [13] Lorz, A., Lorenzi, T., Hochberg, M.E., Clairambault, J., Perthame, B. (2013). Populational adaptive evolution, chemotherapeutic resistance and multiple anti-cancer therapies. *Mathematical Modelling and Numerical Analysis*, 47:377-399.
- [14] Lorenzi, T., Pouchol, C. (2020). Asymptotic analysis of selection-mutation models in the presence of multiple fitness peaks. *Nonlinearity*, 33(11), 5791.
- [15] Meza Guzman, L.G., Keating, L., Nicholson, S.E. (2020). Natural Killer Cells: Tumor Surveillance and Signaling. *Cancers*, 12:952.
- [16] Benoît Perthame. *Transport equations in biology*. Birkhäuser, Boston, 2007.
- [17] Pesce, S., Greppi, M., Grossi, F., Del Zotto, G., Moretta, L., Sivori, S., Genova, C., Marcenaro, E. PD/1-PD-Ls Checkpoint: Insight on the Potential Role of NK Cells. *Frontiers in Immunology*, 10:1242, 2019.
- [18] Pouchol, C., Clairambault, J., Lorz, A., Trélat, E. (2018). Asymptotic analysis and optimal control of an integro-differential system modelling healthy and cancer cells exposed to chemotherapy. *Journal de Mathématiques Pures et Appliquées*, 116, 268-308.
- [19] Pouchol, C. (2015). *Modelling interactions between tumour cells and supporting adipocytes in breast cancer* (Doctoral dissertation, UPMC).
- [20] Pradeu. T. (2019). *Philosophy of immunology*. Cambridge University Press.
- [21] Robert, C., Schachter, J., Long, G. V., Arance, A., Grob, J. J., Mortier, L., Larkin, J. (2015). Pembrolizumab versus ipilimumab in advanced melanoma. *New England Journal of Medicine*, 372(26), 2521-2532.
- [22] Schreiber, R. D., Old, L. J., Smyth, M. J. (2011). Cancer Immunoediting: Integrating Immunity's Roles in Cancer Suppression and Promotion. *Science*, 331(6024), pp. 1565-1570.
- [23] Shen, S., Clairambault, J.(2020). Cell plasticity in cancer cell populations (review) [version 1; peer review: 2 approved]. *F1000Research* 2020 9(F1000 Faculty Rev), 635-650, DOI:10.12688/f1000research.24803.1.
- [24] Stewart, T. H. (1996). Immune mechanism and tumour dormancy. *Revista Medicina*, 56(1), 74.
- [25] Takahashi, K., Yamanaka, S. (2006) Induction of Pluripotent Stem Cells from Mouse Embryonic and Adult Fibroblast Cultures by Defined Factors. *Cell* 126:663-676.
- [26] Van Der Leun, A.M., Thommen, D.S., Schumacher, T.N. (2020). CD8<sup>+</sup> T cell states in human cancer: insights from single-cell analysis. *Nature Reviews Cancer*, 20(4):218-232.
- [27] Zhang, H., Dai, Z.Y., Wu, W.T., Wang, Z.Y., Zhang, N., Zhang, L.Y., Zeng, W.J., Liu Z.X., Cheng, Q. (2021). Regulatory mechanisms of immune checkpoints PD-L1 and CTLA-4 in cancer. *Journal of Experimental and Clinical Cancer Research*, 40:184.